

Measurement of Valley Kondo Effect in a Si/SiGe Quantum Dot

Mingyun Yuan, Zhen Yang, Chunyang Tang, and A. J. Rimberg*

Department of Physics and Astronomy,

Dartmouth College, Hanover, New Hampshire 03755, USA

R. Joynt, D. E. Savage, M. G. Lagally, and M. A. Eriksson

University of Wisconsin-Madison, Madison, Wisconsin 53706, USA

(Dated: December 6, 2012)

Abstract

We report measurement of the valley Kondo effect in a Si/SiGe quantum dot. The Kondo peaks in two consecutive Coulomb diamonds show unusual behavior in a magnetic field that we interpret as arising from the valley degree of freedom. In one diamond two Kondo peaks due to screening of the valley index exist at zero field, revealing a zero-field valley splitting of 0.28 meV. In a finite field the peaks broaden and coalesce due to Zeeman splitting. In the other diamond, a single resonance persists at zero bias for non-zero field, a phenomenon characteristic of valley non-conservation in tunneling.

The valley degree of freedom of conduction band electrons is one of several intriguing properties distinguishing silicon from III-V materials. The six-fold valley degeneracy in bulk Si is reduced to two-fold in Si/SiGe heterostructures due to the confinement of electrons in a two-dimensional electron gas (2DEG). The resulting valley splitting Δ in strained Si quantum wells has been studied using conventional transport [1, 2] and is typically of order 0.1 meV. A particularly interesting manifestation of valley physics would be the valley Kondo effect. The spin 1/2 Kondo effect comprehensively studied in GaAs quantum dots (QD) [3–9] is usually observed when there is an odd number of electrons in the QD, in which the spin of an unpaired electron is screened by spins in the leads to form a singlet, resulting in a conductance resonance at zero dc bias. When spin degeneracy is lifted by a magnetic field B , the spin-Kondo resonance splits into two peaks at $eV_{SD} = \pm g\mu_B B$, g being the Landé factor and μ_B the Bohr magneton [10]. On the other hand, Kondo effects in Si/SiGe QDs have rarely been reported [11], although there have been recent studies of dopants in a Si fin-type field effect transistor [12]. This is perhaps not surprising, since for the valley Kondo effect to occur, the energy associated with the Kondo temperature T_K must be larger than the valley splitting Δ , i.e. $k_B T_K > \Delta$ where k_B is the Boltzmann constant, a rather stringent condition. Nonetheless, how the valley degeneracy in Si affects the Kondo effect in Si/SiGe QDs has been investigated theoretically [13, 14] and found to share some resemblance with carbon nanotubes [15]. The addition of the valley degree of freedom allows for a new set of phenomena to emerge, since both spin and valley indices can be screened. Measurement of the valley Kondo effect can therefore help probe the nature of valley physics in Si/SiGe QDs, a topic of great importance considering their potential application in quantum computation. In particular, the question of how the valley index of an electron changes as it tunnels on and off a QD can be illuminated.

Here we report measurement of unconventional Kondo effects in a Si/SiGe QD. We observe conductance enhancement in two consecutive Coulomb diamonds, forbidden in a purely spin 1/2 Kondo effect. The resonances disappear as temperature is raised above a few Kelvin. In one diamond there are two peaks at zero magnetic field which coalesce and broaden into a single peak as B is increased. In a successive diamond the resonance persists at zero bias in finite field. We show that these counterintuitive phenomena arise from an interplay between the valley and spin degrees of freedom.

The doped Si/SiGe heterostructure is grown on Si (001) miscut 2 degrees toward (010). The device is fabricated with low-leakage Pd gates [16]. We form a QD with gates T, M, and R (Fig. 1(a)) and measure its differential conductance with lock-in techniques, using an ac bias of $3 \mu\text{V}$. The sample is cooled down to about 60 mK, corresponding to an electron temperature of $T_e \approx 150$ mK and oriented perpendicular to the magnetic field to enhance the valley splitting.

Interesting conductance enhancements appear in the Coulomb blockade region, as shown in the stability diagram of the QD differential conductance G in Fig. 1(b). The x -axis is the dc bias voltage V_{SD} (a slight offset is present). Gates M and R are kept constant, while the voltage V_g on gate T is displayed on the y -axis. There is a lower Coulomb diamond between $V_g \approx -0.85$ and -0.69 V and an upper one starting at $V_g \approx -0.69$ and extending towards the top of the figure. The relatively large size of this lower diamond (V_{SD} between ± 3 mV) suggests that the QD is in the few-electron regime. It also shows co-tunneling features consisting of two roughly vertical regions of enhanced conductance for $V_{\text{SD}} < -0.5$ mV and $V_{\text{SD}} > 0.9$ mV that depend only weakly on V_g . The inelastic co-tunneling is due to virtual transitions to an excited state with excitation energy of about 0.8 meV, indicating that it involves a change in orbital state rather than valley state, for which the excited state energies are typically < 0.2 meV. The co-tunneling feature has important implications for electron number N in the QD. The addition energy $E(N)$ is given by $E(N) = U(N)$ for N odd and $E(N) = U(N) + \epsilon(N)$ for N even due to spin degeneracy, where $U(N)$ is the charging energy and $\epsilon(N)$ is the single-particle energy level spacing in the QD. In few-electron QDs, $\epsilon(N) > U(N)$ is typically satisfied. Consequently for N odd, $\epsilon(N) > E(N)$ and inelastic co-tunneling is not observed inside the Coulomb diamond, while for N even $\epsilon(N) < E(N)$ is always satisfied, allowing co-tunneling to be observed [17]. Thus the presence of the co-tunneling in the lower diamond identifies it as corresponding to an even-electron-number state. The upper diamond must therefore correspond to an odd-electron-number state. We refer to the upper (lower) diamond as the odd(even)-number diamond. The Kondo effect in Si/SiGe QDs is forbidden for $N = 4m, m = 0, 1, 2, \dots$ [14] since the spin and valley states for a particular orbital state are filled. Therefore, the even-number diamond corresponds to $N = 4m + 2$ while the odd-number diamond corresponds to $N = 4m + 3$.

The temperature dependence of the resonances in the odd- and even-number diamonds is shown in Fig. 2(a) and (b), respectively, while their magnetic field dependence is shown in Fig. 2(c) and (d). As can be seen in Fig. 2(a) and (b), the resonances weaken as the temperature increases and vanish for $T > 1.8$ K, verifying the presence of Kondo physics. There are several notable aspects of these resonances that contradict the spin 1/2 Kondo picture, such as a split resonance that coalesces into a single peak in the odd-number diamond and a single resonance in the even-number diamond that does not shift in V_{SD} as B is increased. These seemingly counterintuitive phenomena are indicators of valley Kondo physics in our QD.

In the odd-number diamond, we find two conductance peaks, one on each side of zero dc bias. Their position with respect to V_{SD} stays mostly the same within the diamond. We fix $V_g = -0.58$ V, varying the temperature (Fig. 2(a)) and magnetic field (Fig. 2(c)). At $T_e \approx 150$ mK, the two peaks are clear. As temperature is raised, the peaks broaden and their height decreases. At 1.2 K only a single broadened peak can be resolved and it eventually becomes difficult to discern at 1.8 K. The data in Fig. 2(a) reveals two characteristic temperatures: $T_{K1} \approx 2.4$ K for the Kondo feature to appear and $T_{K2} \approx 1$ K to resolve the individual valley Kondo peaks. This result is consistent with theoretical calculations for a Si QD with valley degrees of freedom [13].

Turning to the field dependence of these features in Fig. 2(c), as B is increased the two peaks broaden and coalesce, becoming indistinguishable at $B=1$ T. The processes resulting in the Kondo effect for a QD with $N = 4m + 3$ are illustrated in Fig. 3(a). Theory predicts three peaks in the absence of B when the valley index is conserved: a peak at zero bias that involves a spin flip, commonly observed in GaAs QDs; and two valley side peaks that are due to changes in both spin and valley indices as the electrons tunnel through the QD [13]. A magnetic field should split each valley Kondo peak into three peaks, the distance between neighboring peaks being $g\mu_B B$. In Fig. 3(a) two valley states with energy difference Δ are labeled by o and e . Note, however, that since parity is not a good quantum number in the device, the states are not necessarily odd and even in the z -coordinate. The levels in the QD are single-particle picture levels not drawn to scale while Kondo effect is a many-

body phenomenon whose ground state is a complex combination of the occupation number eigenstates of the single-particle levels. The diagrams are meant only to identify the process associated with each resonance. In the upper panel ($B = 0$), the orange arrows correspond to the conventional spin 1/2 Kondo effect that results in a central peak. In contrast, the blue arrows illustrate a process in which an electron occupying the o valley state tunnels off the QD, and another electron from the lead tunnels on to the QD to occupy the e state, resulting in the side peaks. This picture at first sight contradicts our experimental results, which show only two side peaks. One possible explanation is that the missing spin 1/2 process has only two-fold degeneracy, while the valley side peaks each have four-fold degeneracy (two processes screening only the valley index and another two screening both valley and spin indices). The valley Kondo resonances involve more many-body processes, giving rise to strong peaks which obscure the central spin 1/2 resonance. In this picture, the separation in V_{SD} of the two side peaks is twice the zero-field valley splitting Δ in the QD, so $\Delta \approx 0.28$ meV. A magnetic field lifts the spin-degeneracy of each valley state. The process illustrated by the blue arrows in the upper panel of Fig. 3(a) then splits into four. The lower panel shows one of them in which a spin-down electron in the o state tunnels off the QD while a spin-up electron tunnels on to the e state, as indicated by the green arrows, swapping both valley and spin indices. The spin direction can be reversed to represent another process. The other two remain degenerate, swapping only the valley index while preserving the spin index. As a result, the four processes generate three resonances in finite B field.

Motivated by calculations that predict the potential location of resonances [13], we model the resonances by keeping the peaks from valley transitions but omitting the unobserved spin 1/2 center peak. Additional assumptions are made for all processes contributing to the Kondo resonances:

- (i) The valley splitting Δ is slowly varying with the magnetic field compared with the Zeeman splitting and is taken to be constant.
- (ii) The line width of the Kondo resonance depends only on the Kondo temperature T_K , and is taken to be constant for different B values.
- (iii) The conductance G_i contributed by each process decreases with the distance from zero dc bias. We approximate the decrease with a Lorentzian with the same FWHM as the Kondo peak.
- (iv) For bulk Si $g = 2$. However in heterostructures and under the influence of a perpendic-

ular B field, this value can be significantly enhanced [11, 18]. We find the value $g \sim 3$ used in Fig. 3(b) agrees best with the data. Comparing the zero-field line width of the valley Kondo peaks 0.4 mV and the size of splitting $g\mu_B B \approx 0.18$ meV at $B = 1$ T, it is clear that the spin splitting will not be resolved in the experiment.

The line shapes are approximated with

$$G_\Sigma(V_{SD}) = \sum_i G_i \cosh^{-2}(\alpha(V_{SD} - V_i)), \quad (1)$$

where $\alpha = 4.6/\text{mV}$ corresponds to FWHM=0.4 mV and G_i and V_i are the heights and positions of the peaks. The upper panel of Fig. 3(b) shows the result of this simulation for $B = 0$. The blue peaks are separated by 0.56 mV and their FWHM is about 0.4 mV, corresponding to the blue arrows in Fig. 3(a). Their sum G_Σ is the red curve, which resembles the zero-field curve in Fig. 2(c). The green curves, corresponding to the three valley-spin resonances discussed above, add up to the blue curve on the right. The right green curve corresponds to the green arrows in Fig. 3(a). When added, the blue curves on either side of zero dc bias result in the black curve, a broad single peak similar to the black curve in Fig. 2(c). In the lower panel we show the total simulated line shapes at $B = 0$ and $B = 1$ T, which resemble the data in Fig. 2(c).

In the even-number diamond, there is a single resonance at zero bias. As shown in Fig. 2(b) the height of the resonance decreases monotonically with temperature, vanishing at ~ 1.8 K, indicating a Kondo temperature of $T_K \sim 3\text{-}4$ K.

Surprisingly, as B is increased this central resonance neither shifts nor splits, as shown in Fig. 2(d), which is significantly different from any Kondo effect previously reported. In fact, a peak at zero dc bias that persists in a non-zero magnetic field is expected to be a signature of pure valley Kondo effect, associating with a process in which the valley index is not conserved [13, 14]. Theory predicts that the center peak should be accompanied by two side peaks at non-zero bias due to Zeeman splitting. Examples of electron tunneling process through the QD expected to give rise to each peak are shown in Fig. 4(a). For the center peak, an electron in the e state tunnels off the QD and another electron hops from the o state in the lead to the e state in the QD, breaking valley conservation as illustrated by the blue arrows in the upper panel. This peak will persist at zero bias even when B is varied,

since the spin direction remains the same. For the two side peaks, a spin-flip is added. The green arrows in the lower panel illustrates one of such processes for which the valley exchange is the same as the center peak but a spin-up electron is replaced by a spin-down electron.

To compare with theory [14], we again produce a phenomenological simulation, choosing the peaks from transitions with non-conserved valley index and making the same assumptions as in the odd-number case. In the upper panel of Fig. 4(b) we plot the line shapes for $B = 0$, showing a single resonance at zero dc-bias. In the middle panel, the green peaks are the Kondo resonances involving additional spin-flips, ± 0.18 mV away from zero dc-bias for $B = 1$ T while the blue curve remains at the center. The center peak involves the process illustrated in the upper panel of Fig. 4(a) while the side peaks correspond to the lower panel of Fig. 4(a). The black curve is the sum of the three peaks. The final results for $B = 0$ and 1 T are compared in the lower panel, showing that for $B = 1$ T the peak height is reduced and its line width broadened, differing considerably from our data (see Fig. 2(d)). This suggests that in contrast to theoretical expectation, for $B \neq 0$ the center peak involving only valley screening dominates while the side peaks are suppressed. The reason for this behavior is unclear. Two possible explanations suggest themselves. The co-tunneling features at higher V_{SD} , which alter the conductance in the diamond at different B values, further complicate the matter and could reduce the broadening of the line shape. Also, with B perpendicular to the 2DEG, we expect some dependence of the tunneling matrix elements on B .

This center peak is rather unusual. First, it suggests that valley index is not always conserved during tunneling, a subject of some debate [12, 13, 15, 19, 20]. There is a fair chance that hopping between different valley states is allowed due to the miscut in the Si/SiGe heterostructure. Secondly, given a non-zero Δ , the QD electrons must occupy an excited state rather than the ground state viewed in terms of single-particle levels (see Fig. 4(a)). This is allowed energetically since by forming the many-body state with the leads, the system gains energy on the order of $k_B T_K \approx 0.4$ meV, estimated from the FWHM of the central peak, in good agreement with the temperature at which the resonance disappears. Assuming $\Delta \approx 0.28$ meV in this even-number diamond, similar to that in the odd-number diamond, we have $\Delta < k_B T_K$, recovering the condition for the valley Kondo effect to be

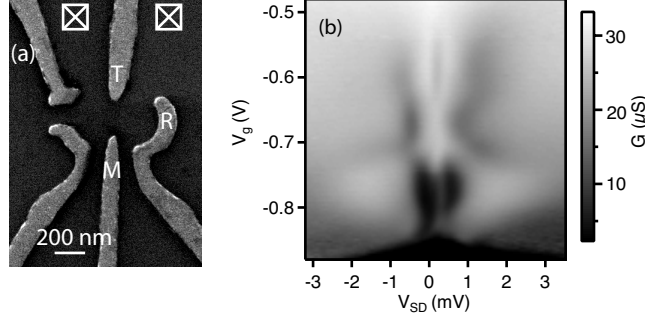


FIG. 1. (a) Electron micrograph of a Si/SiGe QD with identical design to the measured device. Crossed squares represent the ohmic contacts. (b) Stability diagram of differential conductance vs. bias voltage V_{SD} and gate voltage V_g at $B = 0$.

observed.

In conclusion, we have measured valley Kondo effects in a Si/SiGe QD. Kondo peaks that diminish with rising temperature are present in two consecutive Coulomb diamonds. In the odd-number diamond there are two peaks at zero field due to valley screening, revealing a zero-field valley splitting of $\Delta \approx 0.28$ meV. In a magnetic field the peaks broaden due to Zeeman splitting and coalesce. In the even-number diamond a resonance at zero bias persists for non-zero B field, which is a unique valley Kondo effect due to valley non-conservation in tunneling. The experiment demonstrates that the valley degree of freedom in Si enriches the Kondo effect in Si/SiGe QDs.

We would like to thank J. Stettenheim for assistance with the dilution refrigerator. This work is supported at Dartmouth and UW-Madison by the Army Research Office under Grant No. W911NF-12-1-0607 and at Dartmouth by the NSF under Grant No. DMR-1104821.

* ajrimberg@dartmouth.edu

- [1] T. B. Boykin, G. Klimeck, M. A. Eriksson, M. Friesen, S. N. Coppersmith, P. von Allmen, F. Oyafuso, and S. Lee, Appl. Phys. Lett. **84**, 115 (2004).
- [2] S. Goswami, K. A. Slinker, M. Friesen, L. M. McGuire, J. L. Truitt, C. Tahan, L. J. Klein, J. O. Chu, P. M. Mooney, D. W. van der Weide, R. Joynt, S. N. Coppersmith, and M. A.

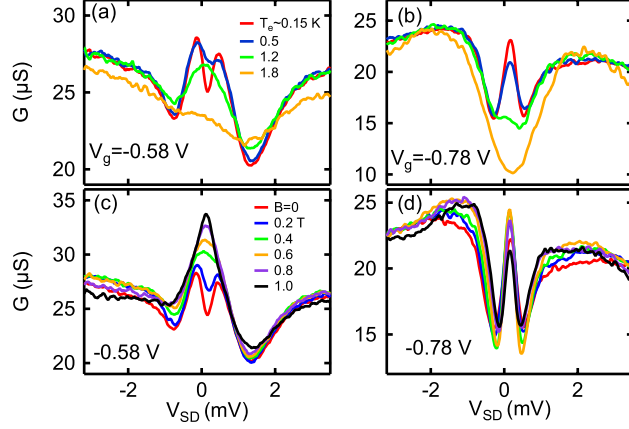


FIG. 2. (a),(b) Zero-field conductance G vs. V_{SD} in the odd(even)-number diamond taken at different temperatures. (c),(d): Magnetic field dependence of the Kondo peaks in (a),(b) at $T_e = 0.15\text{K}$.

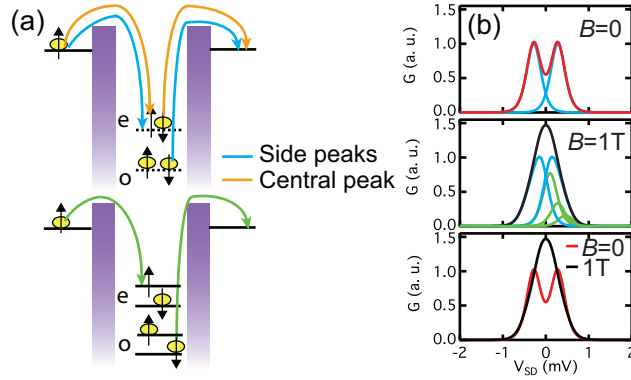


FIG. 3. (a) Upper panel: blue arrows indicate the spin and valley-reversing processes. The process with orange arrows is allowed by symmetry but not observed, possibly due to its weaker contribution. Lower panel: a spin and valley-reversing process in non-zero B . (b) Upper panel: the two blue curves simulating the resonances shown by the blue arrows in (a) add to produce the red curve at $B = 0$ (Eq. (1)). The B dependence of the individual peaks and their sums are shown in the middle panel for $B = 1\text{ T}$. Bottom panel: sums for $B = 0$ and 1 T .

Eriksson, Nat. Phys. **3**, 41 (2007).

[3] D. Goldhaber-Gordon, H. Shtrikman, D. Mahalu, D. Abusch-Magder, U. Meirav, and M. A. Kastner, Nature **391**, 156 (1998).

[4] S. M. Cronenwett, T. H. Oosterkamp, and L. P. Kouwenhoven, Science **281**, 540 (1998).

[5] A. Vidan, M. Stopa, R. M. Westervelt, M. Hanson, and A. C. Gossard,

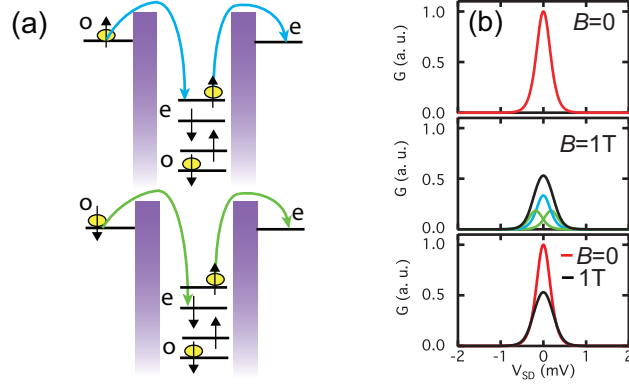


FIG. 4. (a) Upper panel: the valley index changes sign as the electron traverses the QD. The associated center peak in G does not move with B . Lower panel: spin-reversing processes resulting in the side peaks. (A second process for the opposite spin flip is not shown). (b) Upper panel: simulated curve of a single resonance at zero bias for $B = 0$. The black curve in the middle panel is the sum of the blue curve and the two green curves for $B = 1$ T. The blue (green) curves result from processes indicated by the blue (green) arrows in 4(b). Bottom: the total simulated conductance for $B = 0$ and 1 T.

Phys. Rev. Lett. **96**, 156802 (2006).

- [6] S. Sasaki, S. D. Franceschi, J. M. Elzerman, W. G. van der Wiel, S. T. M. Eto, and L. P. Kouwenhoven, Nature **405**, 764 (2000).
- [7] W. G. van der Wiel, S. De Franceschi, J. M. Elzerman, S. Tarucha, L. P. Kouwenhoven, J. Motohisa, F. Nakajima, and T. Fukui, Phys. Rev. Lett. **88**, 126803 (2002).
- [8] A. Kogan, G. Granger, M. A. Kastner, D. Goldhaber-Gordon, and H. Shtrikman, Phys. Rev. B **67**, 113309 (2003).
- [9] G. Granger, M. A. Kastner, I. Radu, M. P. Hanson, and A. C. Gossard, Phys. Rev. B **72**, 165309 (2005).
- [10] Y. Meir, N. S. Wingreen, and P. A. Lee, Phys. Rev. Lett. **70**, 2601 (1993).
- [11] L. J. Klein, D. E. Savage, and M. A. Eriksson, Appl. Phys. Lett **90**, 033103 (2007).
- [12] G. C. Tettamanzi, J. Verduijn, G. P. Lansbergen, M. Blaauboer, M. J. Calderón, R. Aguado, and S. Rogge, Phys. Rev. Lett. **108**, 046803 (2012).
- [13] S.-y. Shiao, S. Chutia, and R. Joynt, Phys. Rev. B **75**, 195345 (2007).
- [14] S.-y. Shiao and R. Joynt, Phys. Rev. B **76**, 205314 (2007).
- [15] P. Jarillo-Herrero, J. Kong, H. S. J. van der Zant, C. Dekker, L. P. Kouwenhoven, and S. D.

- Franceschi, Nature **434**, 484 (2005).
- [16] M. Yuan, F. Pan, Z. Yang, T. J. Gilheart, F. Chen, D. E. Savage, M. G. Lagally, M. A. Eriksson, and A. J. Rimberg, Appl Phys Lett **98**, 142104 (2011).
- [17] S. De Franceschi, S. Sasaki, J. M. Elzerman, W. G. van der Wiel, S. Tarucha, and L. P. Kouwenhoven, Phys. Rev. Lett. **86**, 878 (2001).
- [18] P. Weitz, R. J. Haug, K. von Klitzing, and F. Schäffler, Surf. Sci. **361-362**, 542 (1996).
- [19] M. Friesen and S. N. Coppersmith, Phys. Rev. B **81**, 115324 (2010).
- [20] D. Culcer, X. Hu, and S. Das Sarma, Phys. Rev. B **82**, 205315 (2010).